

The computational approach of designing novel SARS-CoV-2 M^{pro} inhibitors: combined QSAR, molecular docking, and molecular dynamics simulation techniques

Jian-Bo Tong^{*1,2}, Ding Luo^{1,2}, Hai-Yin Xu^{1,2}, Shuai Bian^{1,2}, Xing Zhang, Xue-Chun Xiao^{1,2}, Jie Wang^{1,2}

¹ College of Chemistry and Chemical Engineering, Shaanxi University of Science and Technology, Xi'an 710021, China

² Shaanxi Key Laboratory of Chemical Additives for Industry, Xi'an 710021, China

***Corresponding author:** Jian-Bo Tong^{*1,2}; E-mail: jianbotong@aliyun.com;

Table S1: Compound structure and their experimental IC_{50} and pIC_{50} values

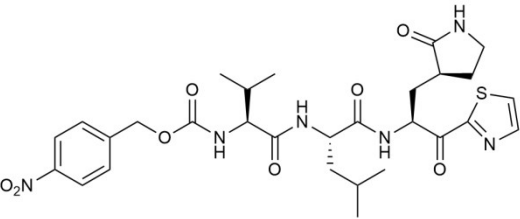
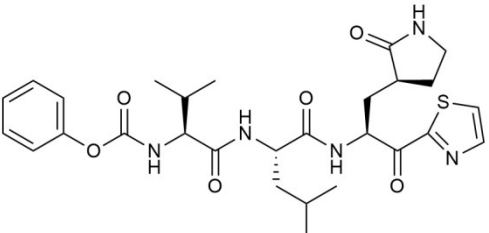
Table S2: Experimental and predicted pIC_{50} with residual of training and test sets based on HQSAR 3-4 and Topomer CoMFA model 2.

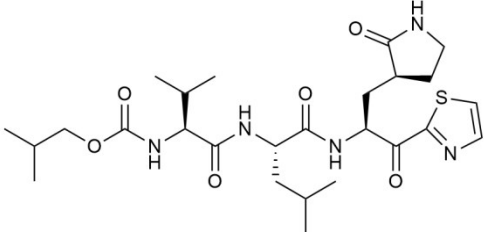
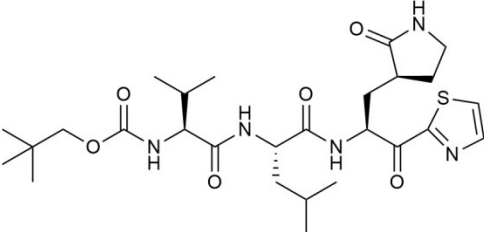
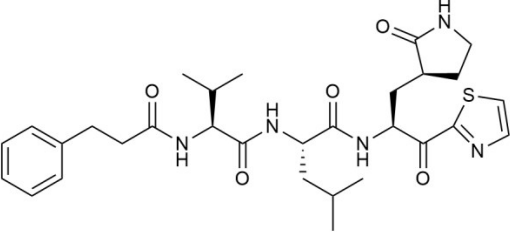
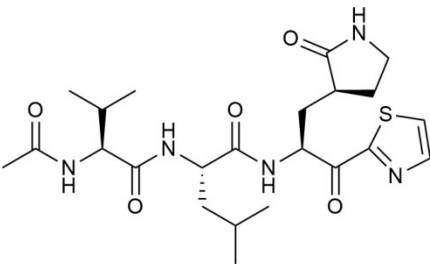
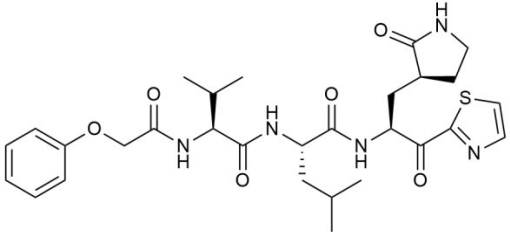
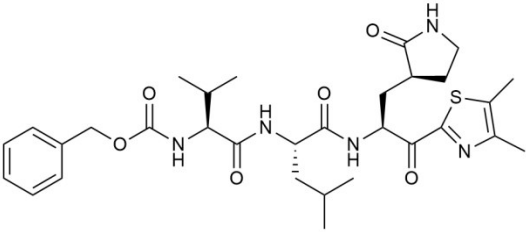
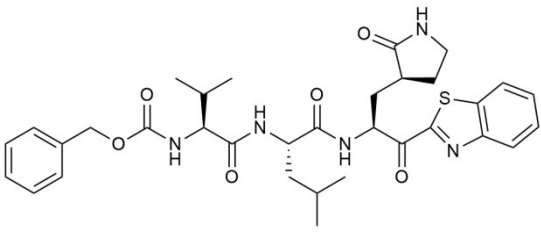
Table S3: Table S3: Y-randomization test of optimal models.

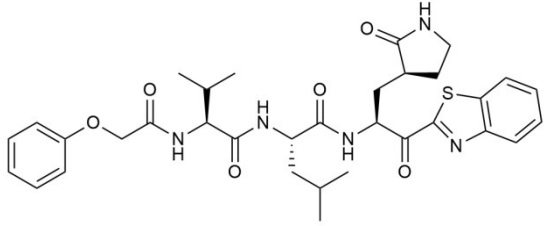
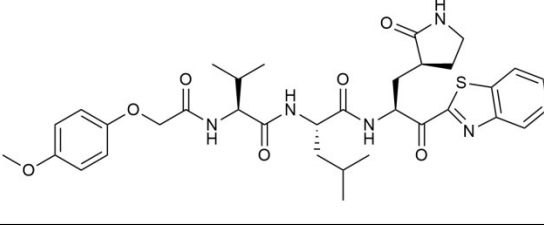
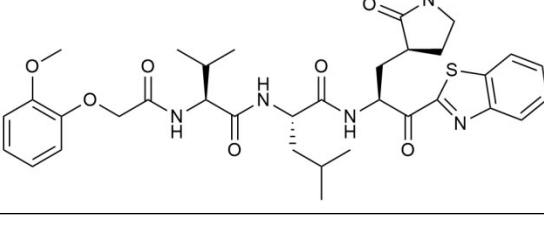
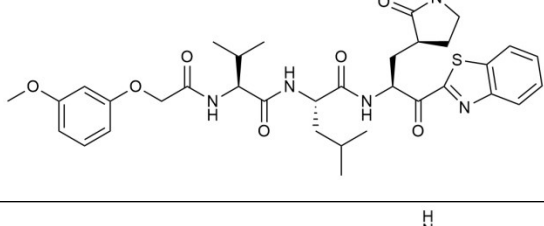
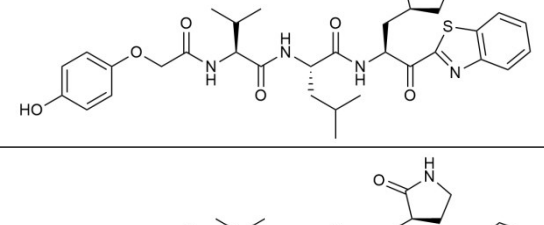
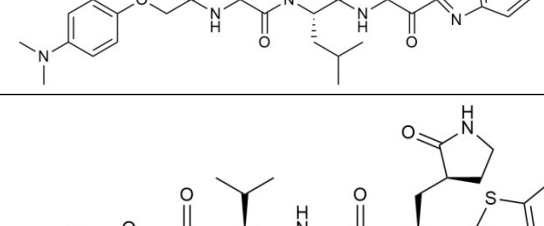
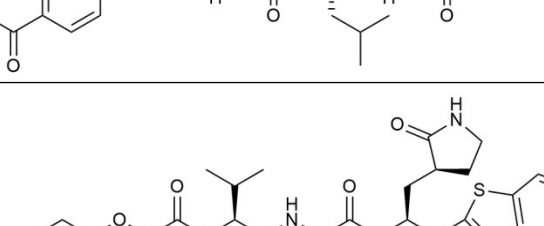
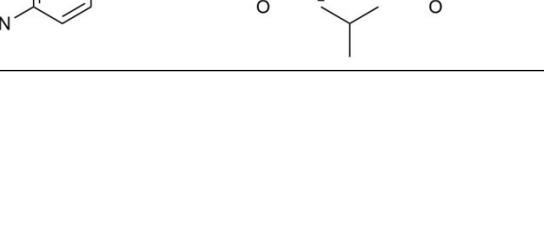
Table S4: Newly designed compounds and predicted activity

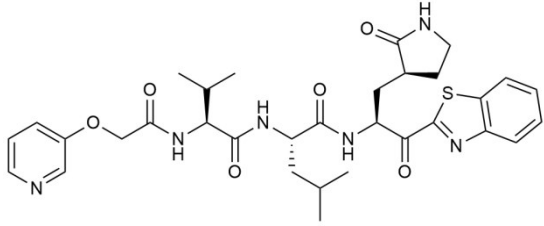
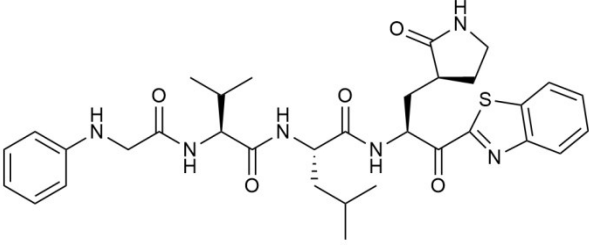
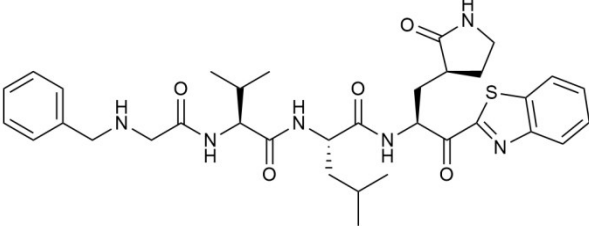
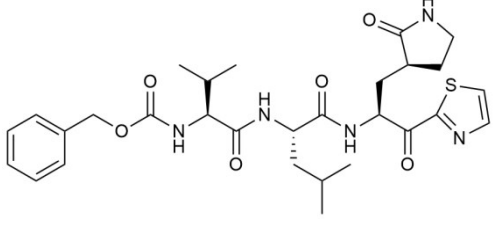
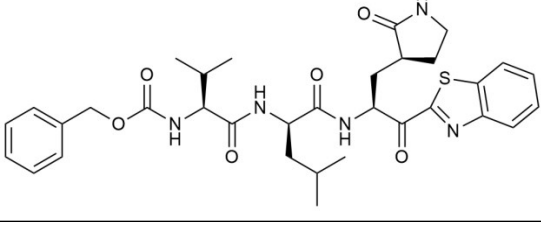
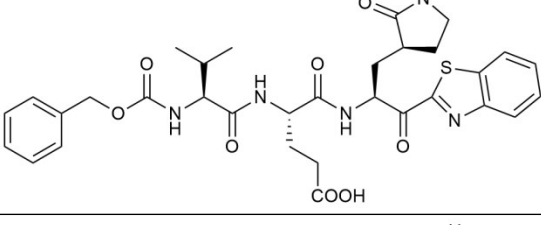
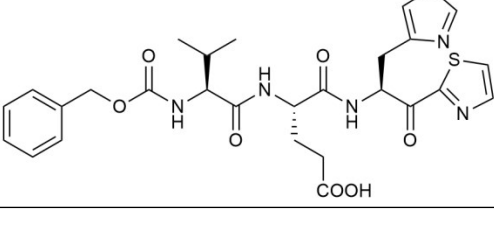
Fig. S1: 2D view of binding conformations and ligand interactions of newly designed compounds at the active site of SARS-CoV-2 M^{pro}

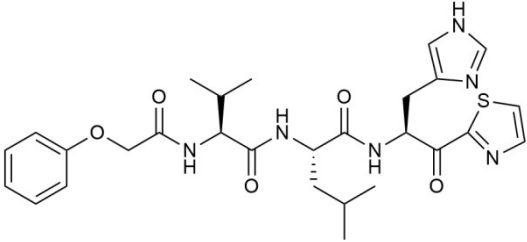
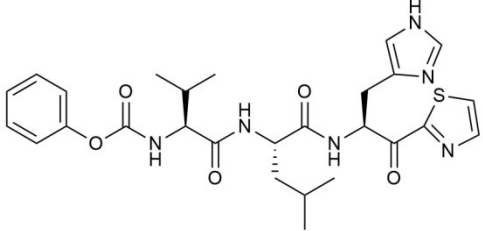
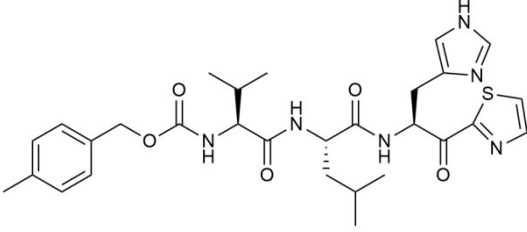
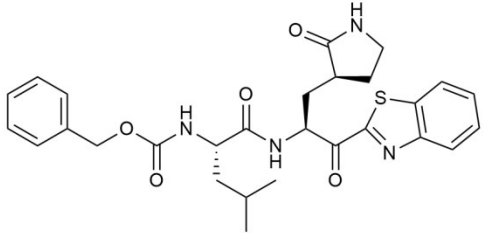
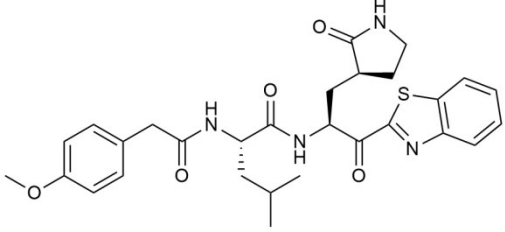
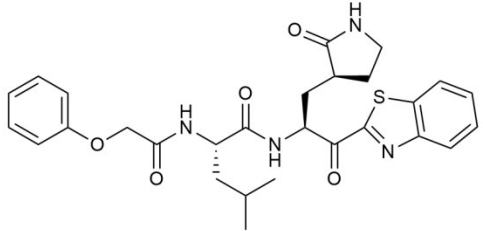
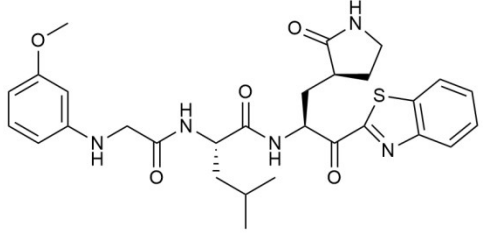
Table S1. Compound structure and their experimental IC_{50} and pIC_{50} values

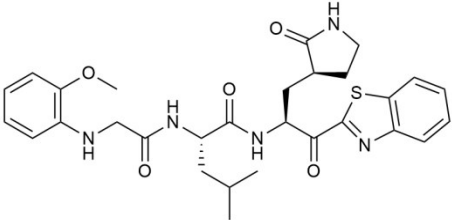
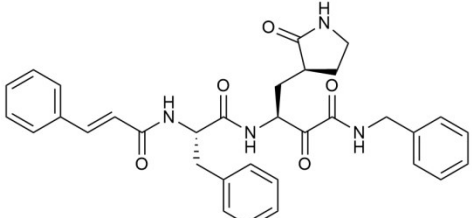
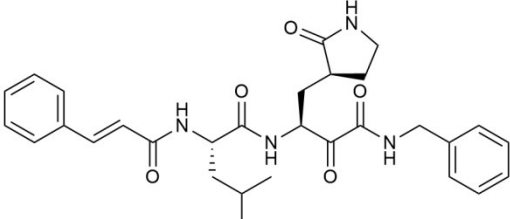
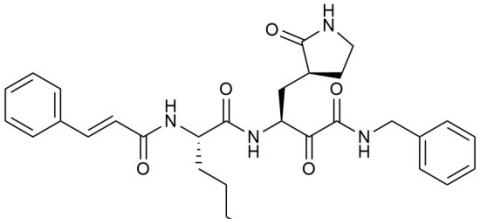
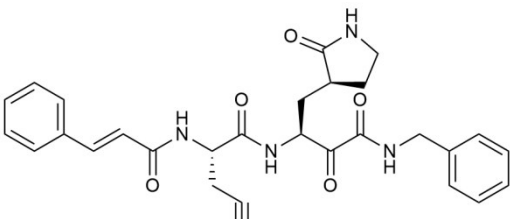
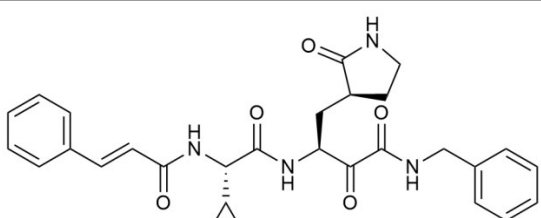
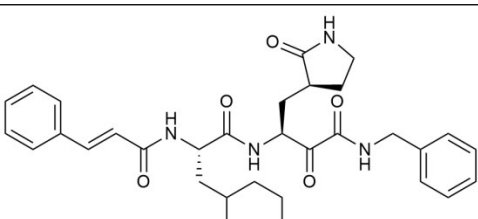
Comp.	structure	IC_{50} (μM)	pIC_{50}
1		36	4.444
2		85	4.071

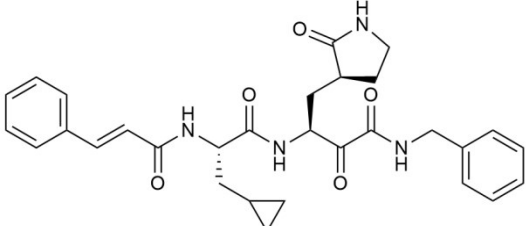
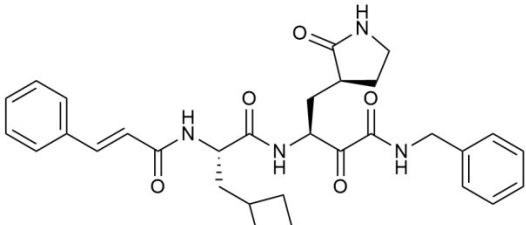
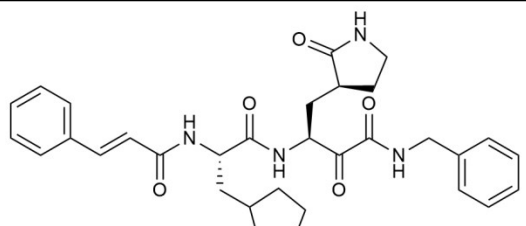
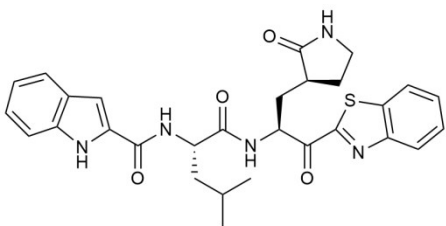
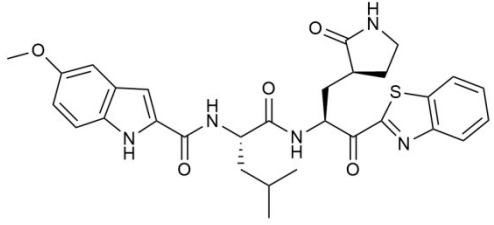
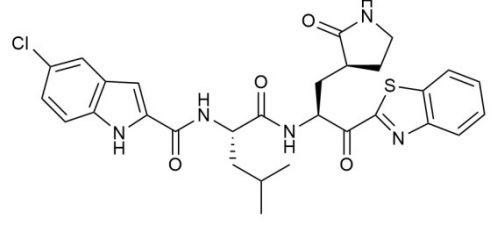
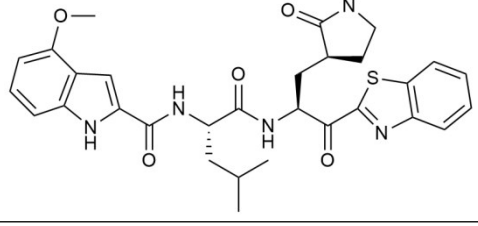
3		250	3.602
4		280	3.553
5		13	4.886
6		24	4.620
7		6.8	5.167
8		2	5.699
9		1.7	5.770

10		2.3	5.638
11		0.92	6.036
12		1.9	5.721
13		0.75	6.125
14		1.2	5.921
15		0.65	6.187
16		1.7	5.770
17		3.4	5.469

18		2.9	5.538
19		1.5	5.824
20		7.5	5.125
21		9.5	5.022
22		1600	2.796
23		1600	2.796
24		260	3.585

25		210	3.678
26		1600	2.796
27		9.5	5.022
28		21.0	4.678
29		43.0	4.367
30		24.0	4.620
31		10.0	5.000

32		14.0	4.854
33		1.95	5.710
34		0.33	6.481
35		8.50	5.071
36		10.68	4.971
37		6.27	5.203
38		0.71	6.149

39		0.24	6.620
40		1.44	5.842
41		1.27	5.896
42		1.50	5.824
43		4.60	5.337
44		4.80	5.319
45		0.74	6.131

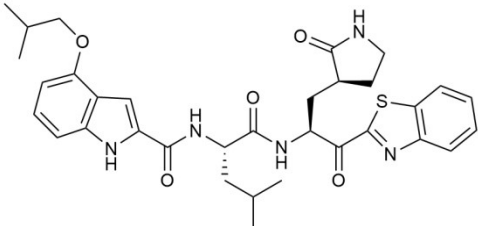
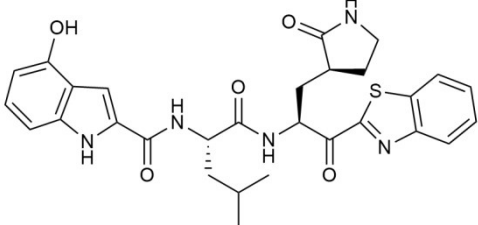
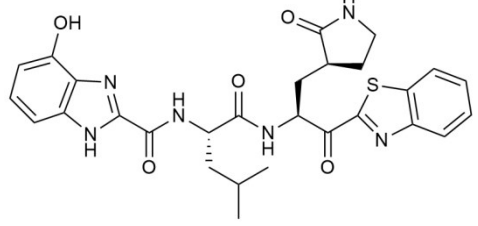
46		5.20	5.284
47		1.50	5.824
48		1.30	5.886

Table S2: Experimental and predicted pIC₅₀ with residual of training and test sets based on HQSAR 3-4 and Topomer CoMFA model 2.

No.	Topomer CoMFA model 2				HQSAR model 3-6		
	Actual pIC ₅₀	Predicted pIC ₅₀	Residual	Fragment contribution		Predicted pIC ₅₀	Residual
				R _a	R _b		
1	4.444	4.371	0.073	1.32	-0.39	4.362	0.082
2*	4.071	3.631	0.442	0.57	-0.39	3.947	0.124
3	3.602	3.510	0.092	0.70	-0.63	3.932	-0.33
4	3.553	3.731	-0.178	-0.73	-0.39	3.607	-0.054
5	4.886	4.395	0.491	1.34	-0.39	4.621	0.265
6*	4.620	3.733	0.887	0.68	-0.39	3.744	0.876
7	5.167	4.921	0.246	1.87	-0.39	4.853	0.314
8	5.699	5.754	-0.055	1.34	0.97	5.954	-0.255
9	5.770	5.385	0.385	1.34	0.60	5.405	0.365
10*	5.638	5.910	-0.272	1.87	0.60	5.638	0.000
11	6.036	5.935	0.101	1.89	0.60	6.049	-0.013
12	5.721	5.883	-0.162	1.84	0.60	5.823	-0.102
13*	6.125	5.944	0.181	1.89	0.60	5.862	0.263
14	5.921	5.935	-0.014	1.89	0.60	5.872	0.049
15	6.187	5.939	0.248	1.90	0.60	6.297	-0.11
16*	5.770	5.886	-0.116	1.84	0.60	5.766	0.004
17	5.469	5.883	-0.414	1.84	0.60	5.363	0.106
18	5.538	5.667	-0.129	1.62	0.60	5.554	-0.016
19*	5.824	5.660	0.164	1.62	0.60	5.595	0.229
20	5.125	4.969	0.156	0.93	0.60	5.131	-0.006

21	5.022	5.387	-0.365	1.34	0.60	5.405	-0.383
22*	2.796	2.789	0.007	1.34	-0.39	3.621	-0.825
23	2.796	3.395	-0.599	-0.26	-0.39	2.803	-0.007
24	3.585	3.824	-0.239	0.77	-0.39	3.562	0.023
25*	3.678	4.347	-0.669	1.28	-0.39	3.759	-0.081
26	2.796	3.026	-0.231	-0.04	-0.39	2.853	-0.058
27*	5.022	3.824	1.198	0.77	-0.39	4.526	0.496
28	4.678	5.041	-0.363	1.00	0.60	4.487	0.191
29	4.367	4.374	-0.007	0.33	0.60	4.314	0.053
30	4.620	4.622	-0.002	0.58	0.60	4.714	-0.094
31*	5.000	4.634	0.366	0.59	0.60	4.806	0.194
32	4.854	4.639	0.215	0.60	0.60	4.900	-0.046
33	5.710	5.721	-0.011	0.94	1.33	5.761	-0.051
34*	6.481	5.858	0.623	1.08	1.33	5.743	0.738
35	5.071	5.366	-0.295	0.60	1.33	5.361	-0.29
36	4.971	4.705	0.266	-0.08	1.33	5.001	-0.03
37	5.203	5.301	-0.098	0.52	1.33	5.795	-0.592
38	6.149	6.176	-0.027	1.39	1.33	6.015	0.134
39	6.620	6.058	0.562	1.28	1.33	6.082	0.538
40	5.842	6.141	-0.299	1.37	1.33	5.964	-0.122
41*	5.896	6.265	-0.269	1.38	1.33	6.074	-0.178
42	5.824	5.686	0.138	1.63	0.60	5.772	0.052
43	5.337	5.511	-0.174	1.46	0.60	5.750	-0.413
44	5.319	5.390	-0.071	1.34	0.60	5.313	0.006
45	6.131	5.987	0.144	1.94	0.60	6.140	-0.009
46*	5.284	5.750	-0.506	1.75	0.60	6.050	-0.766
47	5.824	5.928	-0.104	1.88	0.60	5.910	-0.086
48	5.886	5.674	0.212	1.63	0.60	5.864	0.022

[a]: Randomly selected as the test set

Table S3: Y-randomization test of optimal models.

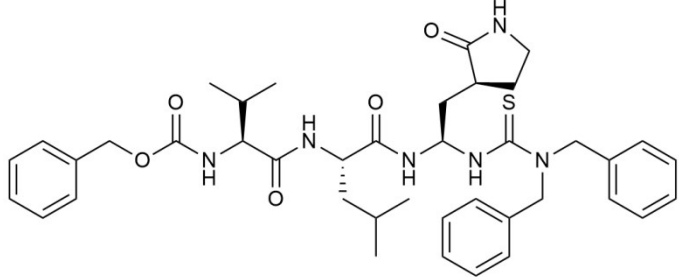
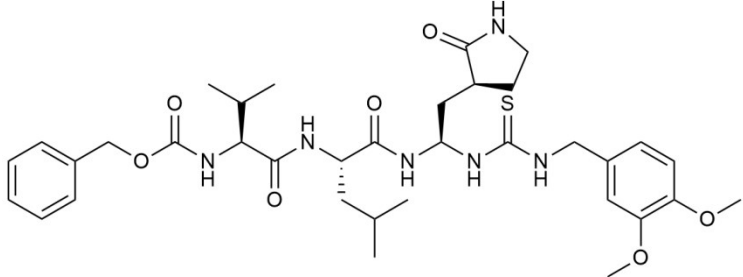
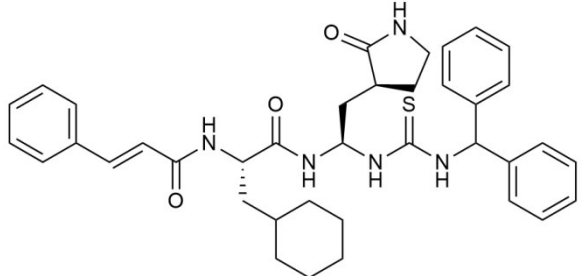
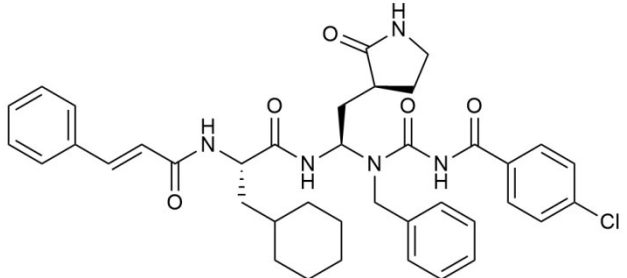
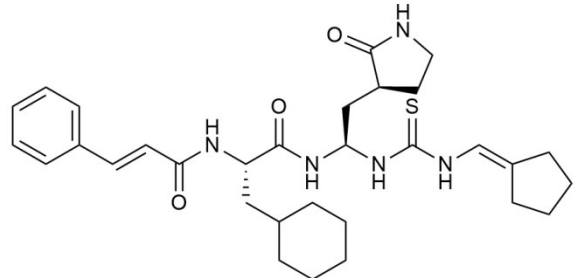
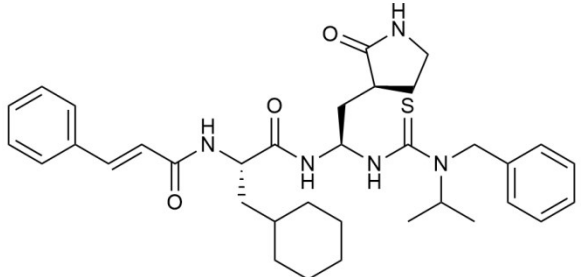
Y-random Iteration	Topomer CoMFA 2		HQSAR3-6	
	r^2	q^2	r^2	q^2
1	0.157	-0.847	0.017	-0.352
2	0.174	-0.367	0.205	-0.072
3	0.307	-0.544	0.140	-0.158
4	0.158	-0.423	0.078	-0.411
5	0.324	-0.378	0.069	-0.476
6	0.200	-0.745	0.099	-0.218
7	0.278	-0.207	0.055	-0.310
8	0.453	-0.744	0.090	-0.191
9	0.237	-0.336	0.128	-0.204
10	0.222	-0.455	0.194	-0.048
11	0.426	-0.115	0.052	-0.328

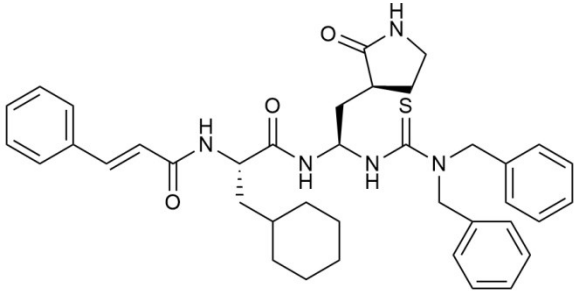
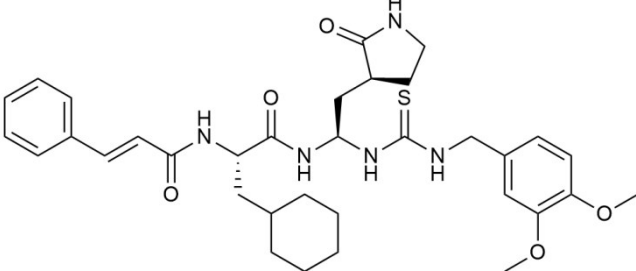
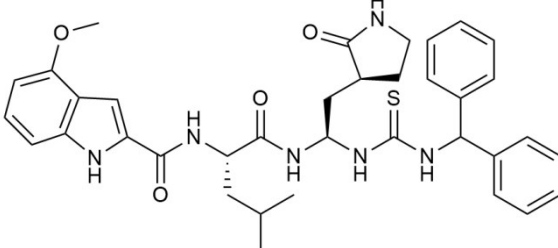
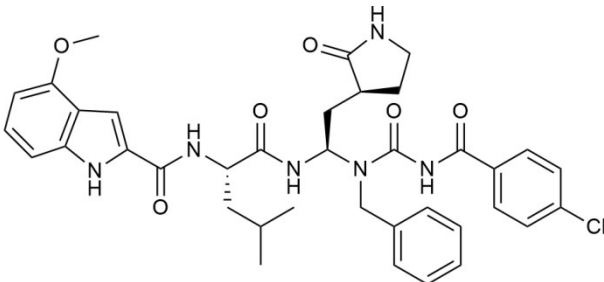
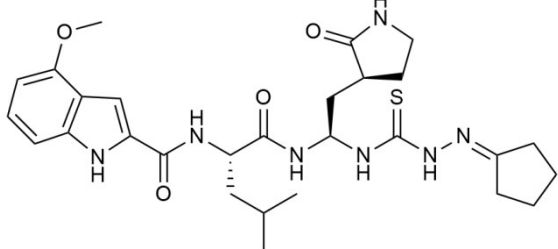
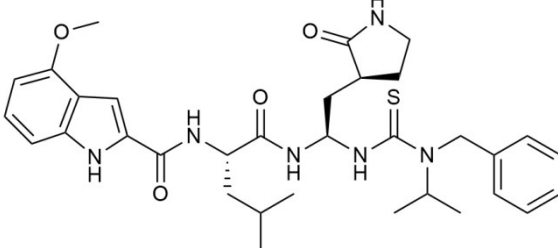
12	0.201	-0.578	0.288	-0.046
13	0.262	-0.639	0.085	-0.256
14	0.351	-0.154	0.025	-0.469
15	0.320	-0.306	0.102	-0.259
16	0.134	-0.521	0.206	0.009
17	0.417	0.0626	0.177	-0.095
18	0.342	-0.288	0.246	-0.175
19	0.231	-0.447	0.209	-0.264
20	0.217	-0.690	0.127	-0.176
Non-Random	0.936	0.738	0.955	0.774

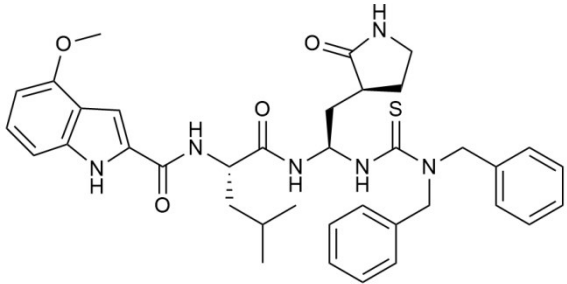
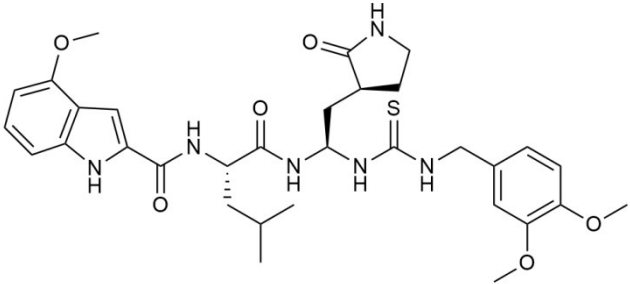
Table S4: Newly designed compounds and predicted activity

Comp.	structure	$pIC_{50}(\text{Pred})_a$	$pIC_{50}(\text{Pred})_b$
15R _a +1		7.07	7.997
15R _a +2		6.91	7.926
15R _a +3		6.97	5.872
15R _a +4		6.94	7.093

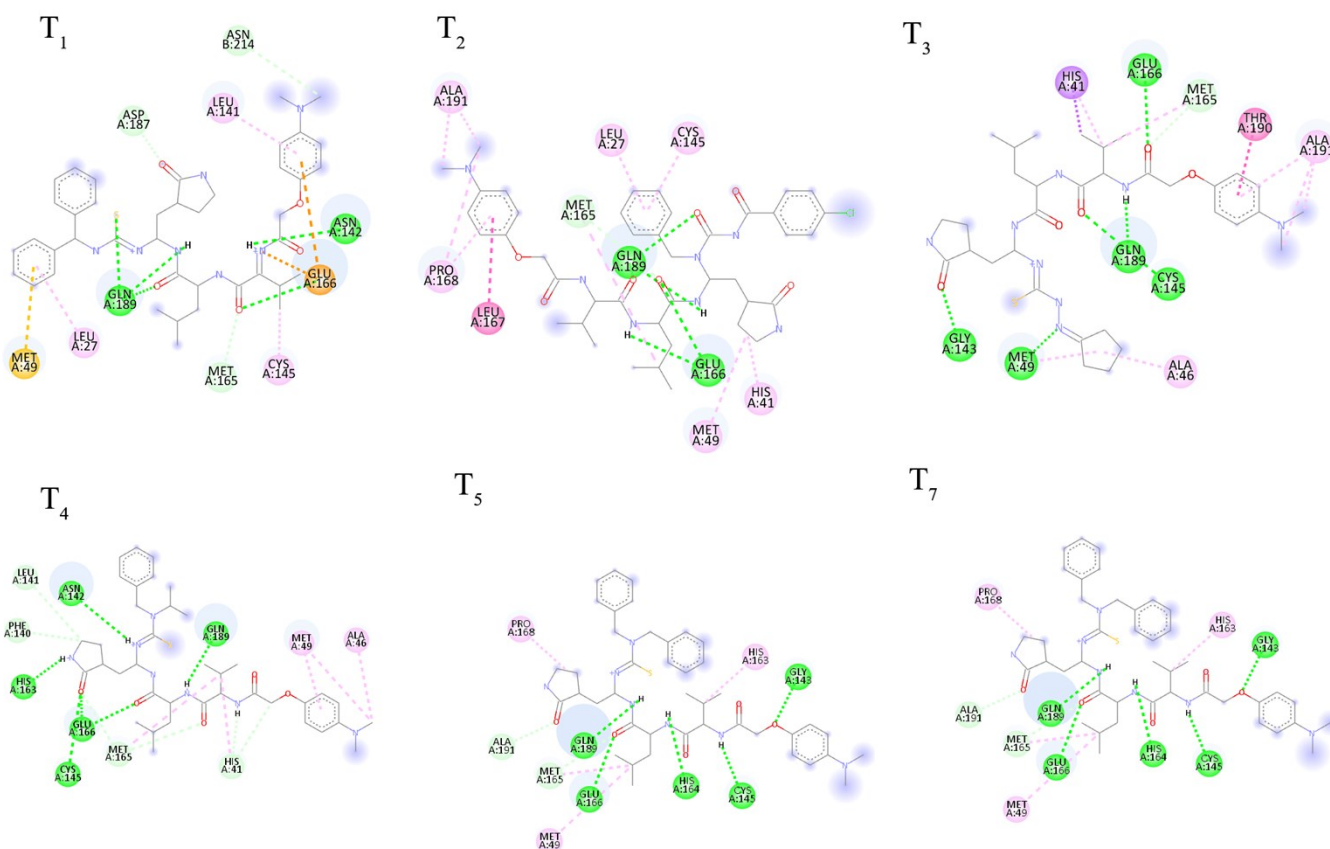
15R _a +5		6.95	7.836
15R _a +6		6.97	6.958
21R _a +1		6.52	7.249
21R _a +2		6.35	7.177
21R _a +3		6.42	5.124
21R _a +4		6.38	6.344

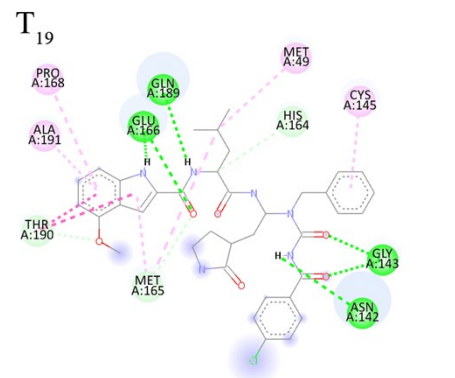
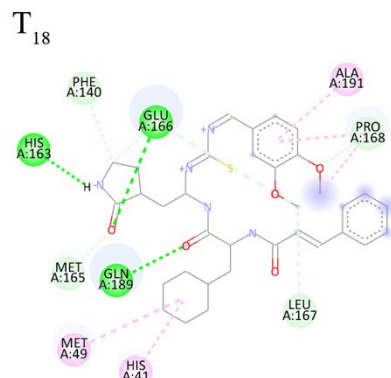
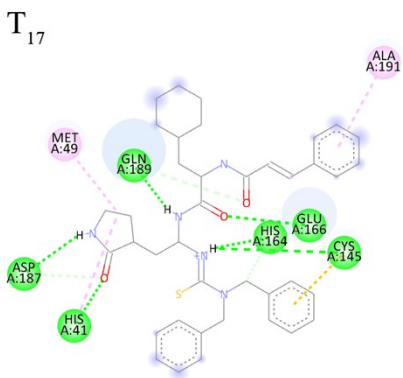
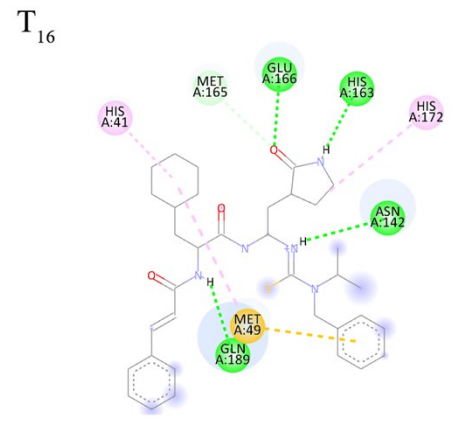
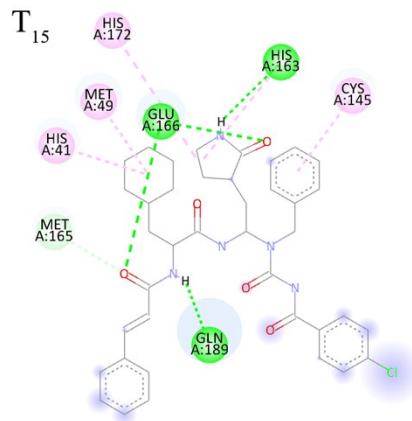
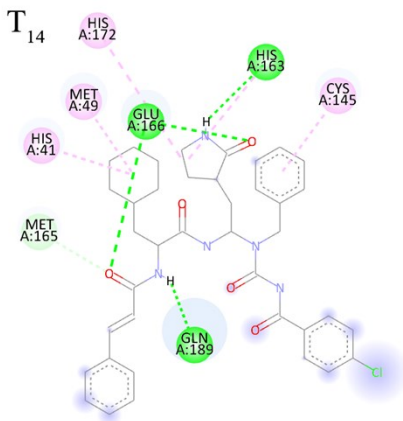
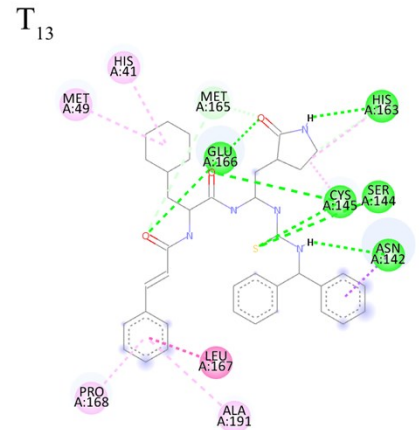
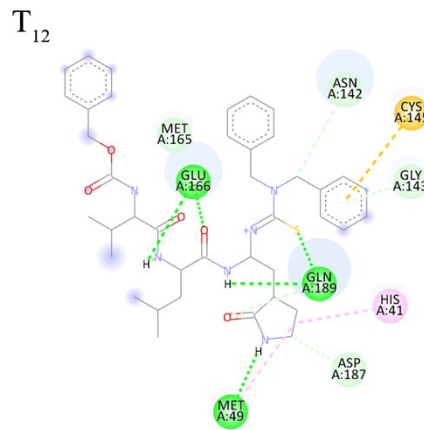
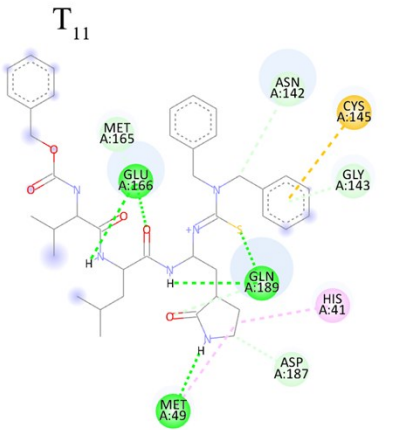
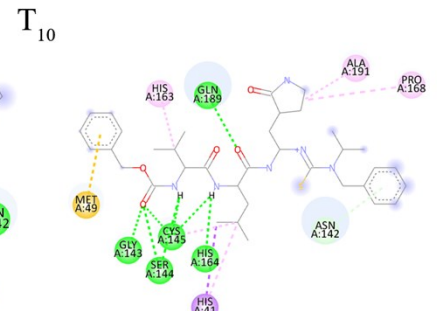
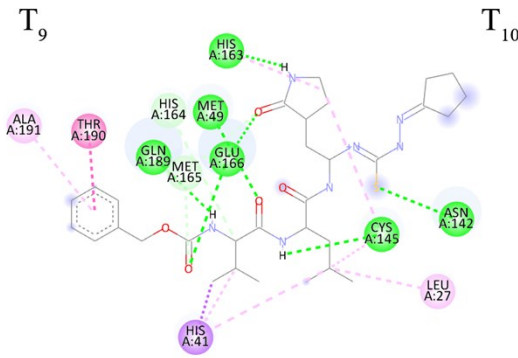
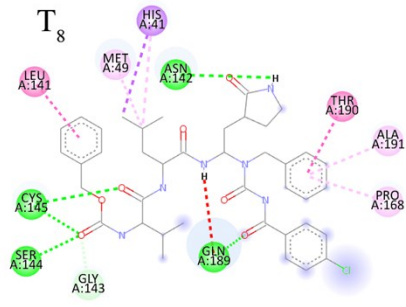
21R _a +5		6.39	7.087
21R _a +6		6.41	6.209
38R _a +1		6.57	7.213
38R _a +2		6.41	7.141
38R _a +3		6.47	5.088
38R _a +4		6.44	6.308

38R _a +5		6.45	7.051
38R _a +6		6.47	6.173
45R _a +1		7.12	7.857
45R _a +2		6.95	7.785
45R _a +3		7.02	5.731
45R _a +4		6.99	7.695

45R _a +5		6.99	7.695
45R _a +6		7.01	6.817

[a]: predicted by Topomer CoMFA model 2; [b]: predicted by HQSAR model 3-4;





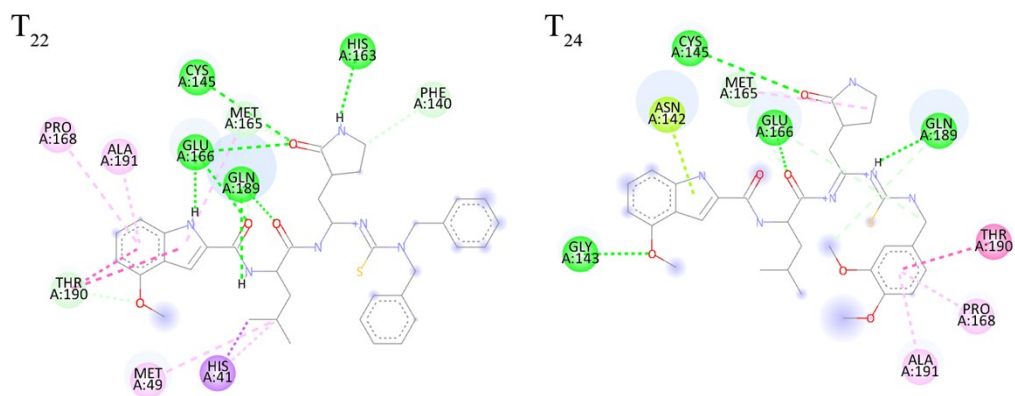


Fig S1: 2D view of binding conformations and ligand interactions of newly designed compounds at the active site of SARS-CoV-2 M^{pro}.